

Spin Adapted versus Broken Symmetry Approaches in the Description of Magnetic Coupling in Heterodinuclear Complexes

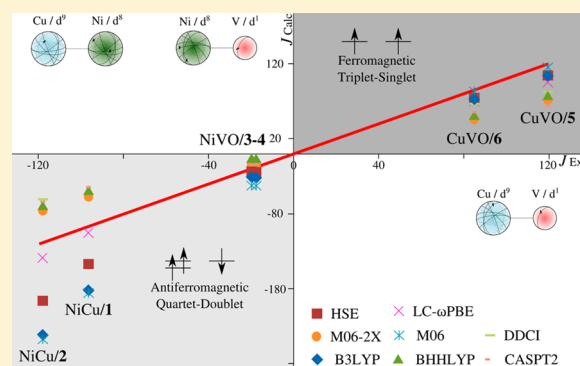
Ramon Costa,^{†,‡} Rosendo Valero,[§] Daniel Reta Mañeru,^{†,||} Ibérico de P. R. Moreira,^{†,||} and Francesc Illas^{*,†,||}

[†]Institut de Química Teòrica i Computacional (IQTCUB), [‡]Departament de Química Inorgànica, and ^{||}Departament de Química Física, Universitat de Barcelona, C/Martí i Franquès 1, E-08028 Barcelona, Spain

[§]Center for Superfunctional Materials, Department of Chemistry, School of Natural Science, Ulsan National Institute of Science and Technology (UNIST), UNIST-gil 50, Ulsan 689-798, Korea

S Supporting Information

ABSTRACT: The performance of a series of wave function and density functional theory based methods in predicting the magnetic coupling constant of a family of heterodinuclear magnetic complexes has been studied. For the former, the accuracy is similar to other simple cases involving homodinuclear complexes, the main limitation being a sufficient inclusion of dynamical correlation effects. Nevertheless, these series of calculations provide an appropriate benchmark for density functional theory based methods. Here, the usual broken symmetry approach provides a convenient framework to predict the magnetic coupling constants but requires deriving the appropriate mapping. At variance with simple dinuclear complexes, spin projection based techniques cannot recover the corresponding (approximate) spin adapted solution. Present results also show that current implementation of spin flip techniques leads to unphysical results.



1. INTRODUCTION

One of the most active areas in contemporary coordination chemistry is the research on molecular magnetism triggered by the possibility to build nanoscale magnetic devices.¹ From a fundamental point of view, this field of research focuses on the study of the exchange coupling interactions between unpaired electrons associated with different metal centers that produce nonmetallic materials with new magnetic properties.² Many efforts have been devoted to the preparation, characterization, and study of such polynuclear complexes with the aim of understanding and controlling their magnetic and electronic properties in order to prepare new materials with applications in electronic and optical devices.³

Progress in this field has been based in establishing magnetostructural correlations for simple systems, paying attention to the nature and oxidation state of the transition metal centers (including the lanthanides), their coordination geometry, and the kind and disposition of the bridging ligands.^{4,5} After analyzing the wide variety of magnetic compounds obtained so far, it has been possible to design and synthesize more complex and efficient systems. Nevertheless, most of the major improvements such as single molecule magnets (SMMs) have been largely achieved through empirical work.⁶ SMMs are metal–organic molecular compounds that show superparamagnetism below a certain “blocking” temperature at the molecular scale.⁷ These systems do not show, in general, collective long-range magnetic order

(i.e., negligible intermolecular magnetic coupling) and the molecular elements consist of a few magnetic centers showing zero-field splitting (ZFS) that provokes a strong anisotropy and significant intramolecular exchange interactions.

From a structural point of view, molecular based magnets are solids formed by molecular building blocks that exhibit ferro-, antiferro-, or ferrimagnetism due to intermolecular interactions between more or less localized magnetic moments. The main difference between these compounds and the standard ferro- or ferrimagnets is related to their low-energy synthesis from wet chemistry (precipitation/crystallization versus metallurgical or electroplating processes) that allows for a series of combinations of different molecular blocks to produce materials with tailored electric, optic, and magnetic properties.⁷ These can be purely organic molecular materials or, most commonly, inorganic or organometallic molecular materials. Finally, it is worth pointing out that purely organic diradicals and polyradicals raised considerable interest because of their possible application in magnetic technologies.^{8,9}

Because of their relative simplicity, binuclear Cu(II) complexes have been the focus in the initial development in molecular magnetism. In these systems, each metallic center contributes to the electronic structure with one unpaired electron localized essentially in one 3d orbital and relativistic

Received: December 18, 2014

effects are almost negligible. Nevertheless, these simple systems exhibit a broad range of magnetic couplings which go from strong ferro- to strong antiferromagnetic, a behavior which can be tuned thanks to a variety of structural features involving coordination geometries, and use of different terminal and bridging ligands. This has permitted to go from mostly empirical⁴ to rational magnetostructural correlations¹⁰ and provided a convenient data set¹¹ to test the accuracy of different types of theoretical methods, either a wave function based on density functional theory (DFT),^{12,13} appropriate calculations through exploration of the low-energy electronic states of different multiplicity, or making use of an appropriate mapping. In the case of DFT based methods, this often implies using a broken symmetry solution, and appropriate mappings to spin eigenfunctions have been proposed,^{14,15} as reviewed in some detail in following text.

The simplicity of the mapping procedures encountered in the case of dinuclear Cu(II) complexes makes it easy to directly extrapolate to other cases, as in the cases involving two Ni(II) centers.¹² However, little is known about the validity of these, in principle, simple procedures for use with more complicated cases such as those involving heteronuclear complexes with two or more different metal atoms. In the present work, we use mixed Cu–V and Ni–Cu dinuclear complexes to explore the different possible approaches to predict magnetic coupling in these systems. In particular, we focus on methods involving spin eigenfunctions either at the wave function or DFT levels and, in the latter, we analyze broken symmetry solutions and propose pertinent mappings.

2. GENERAL THEORETICAL FRAMEWORK

For many molecular and extended magnetic systems, the magnetic moments are well-localized on a given atom or group of atoms, referred to as magnetic centers or magnetic sites.¹⁶ A simple model to represent the low-energy spectrum of this kind of systems consists of assigning a given effective magnetic moment, S_i , to each magnetic center and making use of a suitable spin Hamiltonian. The possible values of S_i depend on the actual electronic configuration of the magnetic center. Hence, the d^8 configuration of Ni^{2+} in NiO or $KNiF_3$ corresponds to an effective magnetic moment of $S_{Ni} = 1$, whereas in the case of Cu dinuclear complexes $S_{Cu} = 1/2$.^{17,18} The physical description of magnetic coupling, or exchange coupling as it is also often termed, in a broad class of chemical compounds including organic biradicals, inorganic complexes, and ionic solids is based on the use of the well-known phenomenological Heisenberg–Dirac–van Vleck (HDVV) Hamiltonian^{17,18} as in eq 1. This Hamiltonian describes the isotropic interaction between localized magnetic moments S_i and S_j as

$$\hat{H}^{HDVV} = - \sum_{\langle i,j \rangle} J_{ij} \hat{S}_i \cdot \hat{S}_j \quad (1)$$

where J_{ij} constants give the magnitude and type of interaction between S_i and S_j localized spin moments and the $\langle i,j \rangle$ symbol indicates that the sum extends to nearest-neighbor interactions only. It is worth pointing out that the magnetic interactions in the HDVV Hamiltonian are of a purely (relativistic) quantum mechanical nature and, in general, much stronger than classical interactions between magnetic dipoles. In eq 1, a positive value of J_{ij} corresponds to a ferromagnetic interaction thus favoring a situation with parallel spins. The set $\{J_{ij}\}$ of parameters (their

number and magnitude) defining the HDVV Hamiltonian characterizes the magnetic ordering of the system and permits one to describe the lowest part of the excitation spectra of magnetic systems. The sign and magnitude of the relevant (i.e., large enough) J_{ij} parameters result from the particular electronic structure that, at the same time, determines the stable molecular or crystal structure of the system. Hence, the magnetic order and the crystal structure of the system are consequences of the actual electronic distribution. Nevertheless, one must advert that in some cases a general spin Hamiltonian containing additional terms may be needed.¹⁹

The approach described previously may seem an empirical one, but there is overwhelming evidence that the HDVV Hamiltonian appropriately describes the low-energy spectrum of magnetic systems which, in turn, represents a fundamental input for the design and preparation of new compounds with tailored magnetic properties. Clearly, understanding and predicting the $\{J_{ij}\}$ set is of paramount importance. Usually, this set of J_{ij} parameters is extracted from experimental measurements such as magnetic susceptibility curves, heat capacity curves, or neutron diffraction experiments and assumes a given form of the spin Hamiltonian. In this way, trial and error procedures are commonly used to fit results and intuition is invoked to choose the relevant interactions.

To avoid an excess of serendipity and to provide unbiased predictions about the relative importance of the different terms, accurate theoretical studies are needed. Here, it is important to point out that theoretical studies based on ab initio methods of electronic structure or on DFT play a very important role, although they also suffer from some limitations, as commented on later. Rigorously speaking, a fully relativistic formalism should be employed. However, the complexity of the n -electron relativistic problem does not permit one to carry out the required calculations for the systems of interest. Still, one can use the nonrelativistic Hamiltonian and handle magnetic interactions through a proper introduction of spin coordinates and spin symmetry, although the price to be paid is that anisotropy, Dzyaloshinskii–Moriya, spin canting, and similar effects cannot be taken into account.¹⁹ To establish an appropriate link between predictions from the HDVV and from accurate calculations, the low-energy spectrum obtained from both approaches needs to be mapped, thus giving rise to a direct way to extract the exchange couplings, although in some cases the low-energy spectrum is not enough and effective Hamiltonian theory must be invoked.¹³

The focus of the present work is precisely on the theoretical prediction of magnetic coupling in inorganic complexes with localized magnetic moments where magnetic coupling usually results from electron–electron correlation effects.^{18–21} Nonetheless, it is fair to acknowledge the few efforts toward an ab initio description of magnetic coupling including spin–orbit effects.²² This field has been studied in detail by various authors, and a recent review is available.¹³ The novelty here is in the heteronuclear nature of the magnetic complexes which, as stated in the previous section, introduces nontrivial aspects on the usual mapping procedure,¹² as described in the next section.

3. STRUCTURAL AND MAGNETIC PARAMETERS OF THE SYSTEMS STUDIED

Two antiferromagnetic Cu(II)–Ni(II) systems with CCDC references PAJZAB (compound 1) and PAJZEF (compound 2) have been selected.²³ These antiferromagnetic complexes show

different coordination on the nickel atom, a 6-fold coordinate for the former and a distorted-TBP 5-fold coordinate for the latter, but with the same oxamato bridging ligand and a similar square-planar environment for the Cu(II) ion. The experimentally reported values are $J(\text{PAJZAB}) = -96.3 \text{ cm}^{-1}$ and $J(\text{PAJZEF}) = -117.8 \text{ cm}^{-1}$. We also selected two $\text{VO}^{\text{IV}}\text{Ni}^{\text{II}}$ systems, WIXFOZ (compound 3) and WIXFUF (compound 4),²⁴ which are electronically equivalent to the Cu(II)–Ni(II) ones and of an antiferromagnetic nature, but here one metal is placed at the beginning of the first transition series and the other at the end, in such a way that the magnetic orbitals are very different in energy. The experimental values are $J(\text{WIXFOZ}) = -17.8 \text{ cm}^{-1}$ and $J(\text{WIXFUF}) = -20.0 \text{ cm}^{-1}$.

Finally, we choose two VO(IV)–Cu(II) systems, BIGFAY²⁵ and PUSJOC,²⁶ electronically equivalent to Cu(II) binuclears, and both moderately ferromagnetic. As in the preceding systems, the magnetic orbitals are again well-separated in energy. The BIGFAY complex (compound 5) consists of two ions inside parallel square-pyramidal environments favored by a Schiff-base bichelating ligand providing two phenoxo-type bridges. The PUSJOC complex cation (compound 6) contains both ions in a hexacoordinated environment inside a macrocyclic ligand with similar phenoxo bridges plus a μ_2 -O,O'-acetato. The experimental coupling constants are $J(\text{BIGFAY}) = 118 \text{ cm}^{-1}$ and $J(\text{PUSJOC}) = 85 \text{ cm}^{-1}$.

The relevant information regarding these compounds is summarized in Table 1.

Table 1. Cambridge Crystallographic Data Base (CCDB) Names, Experimental J Values (cm^{-1}), and Reference of the Molecular Systems Studied

complex	CCDB name	J	ref
1	PAJZAB	−96.3	23
2	PAJZEF	−117.8	23
3	WIXFOZ	−17.8	24
4	WIXFUF	−20.0	24
5	BIGFAY	118	25
6	PUSJOC	85	26

4. EXTENDING THE MAPPING APPROACH TO HETERODINUCLEAR COMPLEXES

a. Case of Spin Eigenfunctions. For a Cu(II)–Cu(II) system, the two unpaired electrons can couple in either a triplet state (parallel alignment) or a singlet state (antiparallel alignment). The relative disposition and energy difference between both states determines the ground state. Hence, a ferromagnetic coupling results in a triplet (T) ground state whereas antiferromagnetic coupling results in singlet (S) ground state. In this simple case, the singlet–triplet gap directly determines the J coupling constant (positive or negative, respectively) in the simple HDVV spin Hamiltonian involving now two magnetic centers only

$$\hat{H}^{\text{HDVV}} = -J\hat{S}_1 \cdot \hat{S}_2 \quad (2)$$

with $S_1 = S_2 = 1/2$ and $J = E(S) - E(T)$.¹²

With a similar reasoning, it turns out that for a Ni(II)–Ni(II) (octahedral) system, the two unpaired electrons per center couple in a local triplet state leading to effective $S_1 = S_2 = 1$ magnetic centers. Now S_1 and S_2 can couple into a quintet (Q), a triplet (T), or a singlet (S) state. Depending on the nature of

the ground state (Q or S), one gets ferromagnetic or antiferromagnetic coupling. Again, the coupling constant J (positive or negative for ferro- and antiferromagnetic coupling, respectively) defining the two-center HDVV spin Hamiltonian as in eq 2, but with $S_1 = S_2 = 1$, is related to the energy difference between spin states, so that $J = E(S) - E(T)$ and $2J = E(T) - E(Q)$ providing, in addition, a way to check that the low-energy spectrum is described by the HDVV spin Hamiltonian.

In a general case involving dinuclear complexes with S_1 and S_2 localized spins, one can easily show that, taking $S_1 \geq S_2$, the possible values for total S range from $(S_1 + S_2)$ down to $(S_1 - S_2)$ and that

$$E(S) - E(S - 1) = (2S + 1)J \quad (3)$$

which is the well-known Landé rule. For Cu(II)–Ni(II) compounds, where $S_1 = 1/2$ and $S_2 = 1$, one simply gets

$$E(Q) - E(D) = -3J/2 \quad (4)$$

which also holds for the case of VO(IV)–Ni(II) complexes, magnetically equivalent to Cu(II)–Ni(II). Finally, for the VO(IV)–Cu(II) complexes, magnetically equivalent to Cu(II)–Cu(II), the singlet–triplet energy difference gives directly J (see Figure 1).

The preceding discussion provides the basis for extracting the J coupling constant from appropriate theoretical calculation of the energy of the different spin states of the system. Clearly, calculations should be accurate enough to resolve small energy differences typically within or below the wavenumber range. Moreover, one must realize that, even if the highest multiplicity state can be expressed by a single determinant wave function, the low spin states involve necessarily a multideterminantal description which often involves more than one configuration state function. Rigorously speaking, multiconfigurational methods are required to describe these electronic states, and, in addition, electron correlation effects are essential to accurately estimate not only the total energy but the total energy differences. For small and medium size systems, this type of calculations can be carried out as described later on.

We now briefly introduce the minimum multiconfiguration form of the relevant electronic states. To this end, we assume that a localized basis set is used with orbitals a_1 and a_2 in center a with local $S_a = 1$ and b_1 in center b with local $S_b = 1/2$. The high spin components of the quartet state can be described as

$$\left| Q, \frac{3}{2} \right\rangle = |a_1 a_2 b_1\rangle \quad (5)$$

or

$$\left| Q, -\frac{3}{2} \right\rangle = |\bar{a}_1 \bar{a}_2 \bar{b}_1\rangle \quad (6)$$

where, as usual, a and \bar{a} denote α and β spin-orbitals, respectively. Similarly, the low spin components of the quartet state are

$$\left| Q, \frac{1}{2} \right\rangle = \frac{1}{\sqrt{3}}(|a_1 a_2 \bar{b}_1\rangle + |a_1 \bar{a}_2 b_1\rangle + |\bar{a}_1 a_2 b_1\rangle) \quad (7)$$

$$\left| Q, -\frac{1}{2} \right\rangle = \frac{1}{\sqrt{3}}(|a_1 \bar{a}_2 \bar{b}_1\rangle + |\bar{a}_1 a_2 \bar{b}_1\rangle + |\bar{a}_1 \bar{a}_2 b_1\rangle) \quad (8)$$

and those of the doublet can be written as

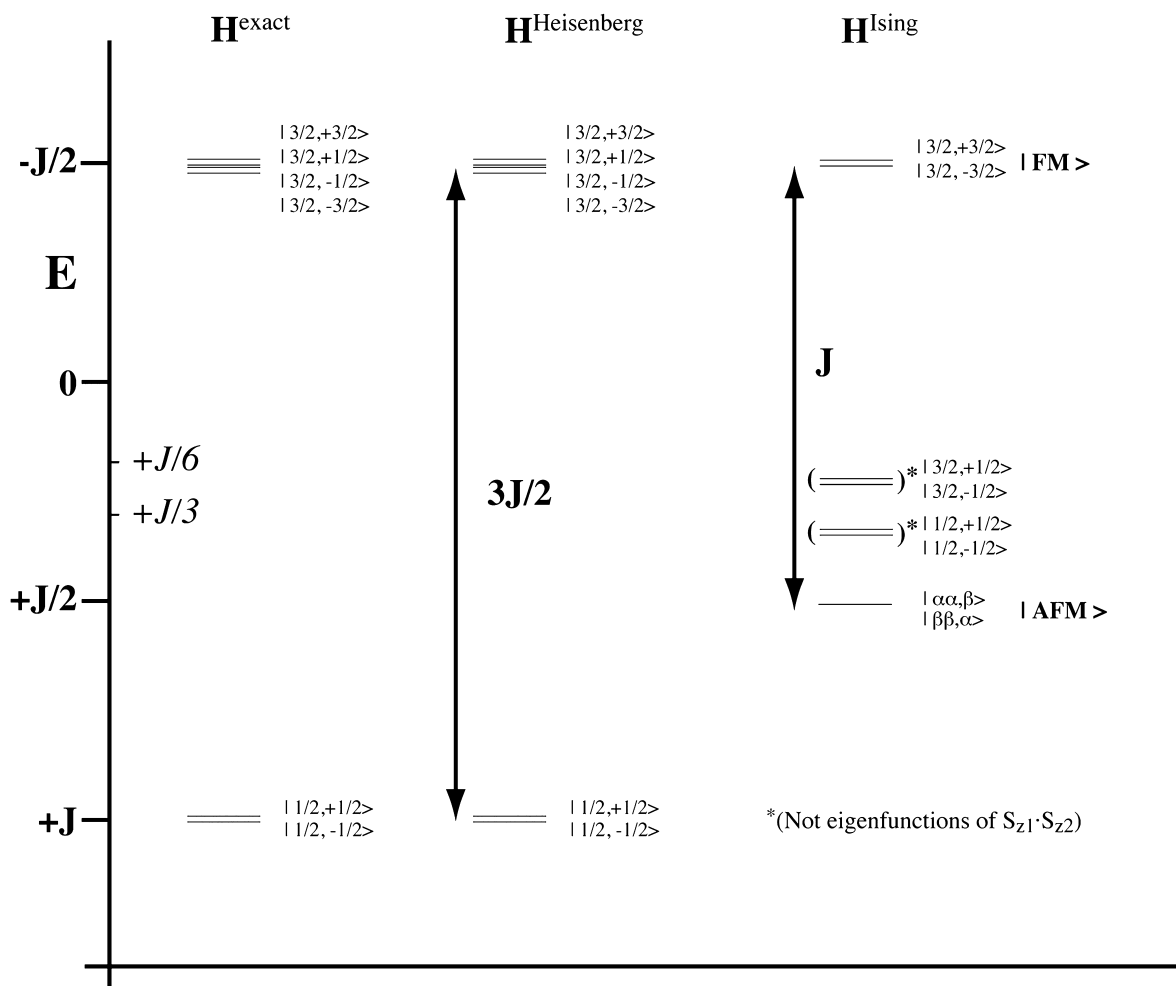


Figure 1. Energy diagram for the eigenstates of the exact, Heisenberg, and Ising model Hamiltonians for a system of local $S_1 = 1$ and $S_2 = 1/2$ interacting spin states with $J < 0$. The states in parentheses indicate that these particular eigenstates of the Heisenberg Hamiltonian are not eigenfunctions of the Ising Hamiltonian and their energy is just an expectation value.

$$\left| D, \frac{1}{2} \right\rangle = \sqrt{\frac{2}{3}} |a_1 a_2 \bar{b}_1\rangle - \frac{1}{\sqrt{6}} (|a_1 \bar{a}_2 b_1\rangle + |\bar{a}_1 a_2 b_1\rangle) \quad (9)$$

$$\left| D, -\frac{1}{2} \right\rangle = \frac{1}{\sqrt{6}} (|a_1 \bar{a}_2 \bar{b}_1\rangle + |\bar{a}_1 a_2 \bar{b}_1\rangle) - \sqrt{\frac{2}{3}} |\bar{a}_1 \bar{a}_2 b_1\rangle \quad (10)$$

From eqs 7–10, it is clear that the doublet states and the $S_z = \pm 1/2$ components of the quartet state include forms that break the local triplet in the $S_a = 1$ center, for instance $|a_1 \bar{a}_2 \bar{b}_1\rangle$, $|\bar{a}_1 a_2 \bar{b}_1\rangle$, $|a_1 \bar{a}_2 b_1\rangle$ and $|\bar{a}_1 a_2 b_1\rangle$. In the following we will show that this fact introduces difficulties in defining the proper mapping to derive the J value from broken symmetry solutions.

b. Case of Broken Symmetry Solutions. For very large systems, explicitly correlated wave function based methods may become unfeasible. Here, one can rely on standard DFT based methods which have proven to provide accurate predictions.^{11,12} Note, however, that these methods are single determinant in nature and the description of the low spin states often involves the use of a broken symmetry (BS) solution. In spite of initial claims that the BS solution approaches the energy of the low spin state, it has been shown that this is not the case,^{12,27} and appropriate mappings are required. This can be easily achieved by realizing that DFT calculated energies are related to the diagonal matrix elements

of the HDVV Hamiltonian and mapping to expectation values rather than to the energy of each spin state. This is consistent with the use of the Ising Hamiltonian, a special case of the HDVV involving diagonal terms only. However, the mapping in terms of expectation values does not require assuming that the J values in both spin Hamiltonians are the same. For Cu dinuclear complexes, J is simply obtained as

$$J = E(S) - E(T) = 2[E(\text{BS}) - E(T)] \quad (11)$$

whereas in the general case one gets

$$J = [E(\text{BS}) - E(\text{HS})]/2S_1 S_2 \quad (12)$$

where HS simply stands for the high spin state. To take into account the inherent spin contamination of the BS solution, Yamaguchi et al.^{28–30} introduced the expectation value of the square of the total spin operator for the HS and BS solutions.

$$J = \frac{E(\text{BS}) - E(\text{HS})}{2(\langle S^2 \rangle_{\text{HS}} - \langle S^2 \rangle_{\text{BS}})} \quad (13)$$

In the cases considered so far, the energy of the low spin states is directly achievable from the appropriate mapping; see for instance Figures 1 and 2 in ref 15. The situation is less clear in the case of heterodinuclear complexes such as those where $S_1 = 1/2$ and $S_2 = 1$ described in the previous section. Obviously,

the description of the high spin state, a quartet (Q) for Cu(II)–Ni(II) and VO(IV)–Ni(II) and a triplet (T) for VO(IV)–Cu(II), poses no problems. However, the situation is less clear for the corresponding low spin states (doublet or open shell singlet, respectively). For the Cu(II)–VO(IV) ferromagnetic systems, the first excited state corresponds to an open shell singlet that we propose to describe by means of a suitable $S_z = 0$ BS solution (here denoted SBS). Here the mapping is as in eq 11, which can be written as

$$J = 2[E(\text{SBS}) - E(T)] \quad (14)$$

For the antiferromagnetic Ni(II)–Cu(II) and Ni(II)–VO(IV) complexes, the quadruplet state corresponds to the first excitation, and the ground state is a multideterminantal doublet where two electrons in the Ni(II) ion remain unpaired and parallel, and in opposite alignment with the unpaired electron of the Cu(II) or VO(IV) moieties. Here, one finds several BS solutions as shown schematically in Figure 1. Note, in addition, that some of the BS solutions are not eigenfunctions of the Ising spin Hamiltonian and, hence, they cannot be compared to the diagonal elements of the HDVV Hamiltonian. This means that these BS solutions cannot be used in the mapping procedure to extract the magnetic coupling constant and one must warn that their use is likely to lead to unphysical results. To solve the puzzle and find the appropriate mapping, one can make use of the information provided by the spin eigenstates in eqs 5–10. Note that from the multiple possible broken symmetry solutions, two cases with $S_z = \pm 1/2$ exist maintaining the local spin on center a as $S_a = 1$. These are $|\text{BS}_1\rangle$ and $|\text{BS}_2\rangle$ which are closely related to the $|a_1 a_2 \bar{b}_1\rangle$ and $|\bar{a}_1 \bar{a}_2 b_1\rangle$ determinants introduced earlier, provided the spatial part of the α and β spin-orbitals are not too different. Obviously, the high spin state solutions are suitable representations of the $|a_1 a_2 b_1\rangle$ and $|\bar{a}_1 \bar{a}_2 \bar{b}_1\rangle$ determinants. Now, note that the $|\text{BS}_1\rangle$ and $|\text{BS}_2\rangle$ solutions are combinations of the $|D, \pm 1/2\rangle$ and $|Q, \pm 1/2\rangle$ wave functions

$$|\text{BS}_1\rangle = 1/\sqrt{3}(|Q, 1/2\rangle + \sqrt{2}|D, 1/2\rangle) \quad (15)$$

$$|\text{BS}_2\rangle = 1/\sqrt{3}(|Q, -1/2\rangle - \sqrt{2}|D, -1/2\rangle) \quad (16)$$

which is reminiscent of the simple singlet–triplet case where, except for spin contaminations, the broken symmetry solution is a mixture of singlet and triplet states.¹⁴ Now, the expectation value of the $|\text{BS}_1\rangle$ and $|\text{BS}_2\rangle$ solutions for the HDVV Hamiltonian can be easily derived as

$$\begin{aligned} \langle \text{BS}_1 | \text{HDVV} | \text{BS}_1 \rangle &= 1/3[E(Q) + 2E(D)] \\ &= 1/3(-J/2 + 2J) \\ &= J/2 \end{aligned} \quad (17)$$

$$\langle \text{BS}_2 | \text{HDVV} | \text{BS}_2 \rangle = \langle \text{BS}_1 | \text{HDVV} | \text{BS}_1 \rangle \quad (18)$$

whereas for the high spin state one has

$$\langle \text{HS} | \text{HDVV} | \text{HS} \rangle = -J/2 \quad (19)$$

Note, assuming that the square of the total spin operator can be computed from the Kohn–Sham density, one also has

$$\langle S^2 \rangle_{\text{BS}_1} = 1/3(\langle S^2 \rangle_Q + 2\langle S^2 \rangle_D) = 1.75 \quad (20)$$

$$\langle S^2 \rangle_{\text{HS}_1} = \langle S^2 \rangle_Q = 3.75 \quad (21)$$

From the preceding discussion it is clear that any possible combination of $|\text{BS}_1\rangle$ and $|\text{BS}_2\rangle$ does not contain any term violating the local triplet $S_a = 1$ on the a center; those components exactly cancel but they are necessary to define the spin states as in eqs 9 and 10. Consequently, it is not possible to univocally define an appropriate spin projector to reconstruct the doublet state from the BS solutions. It is worth pointing out that this is at variance with the homonuclear cases where spin projection reconstructs the appropriate spin state. Figure 1 summarizes the preceding main conclusions and illustrates that, in practice, one can simply use

$$J = E(\text{SBS}) - E(Q) \quad (22)$$

where SBS stands for suitable $S_z = 1/2$ BS solution and Q for the high spin solution representing the quartet state. Finally, note that some of the problems encountered in deriving the preceding mappings for the heterodinuclear complexes were already identified in the case of Ni(II)–Ni(II) complexes, where multiple BS solutions exist, some of which do not have physical meaning.^{12,15} An important difference between Ni(II)–Ni(II) and heteronuclear systems exists. In the first case, the two possible antiferromagnetic BS solutions (i.e., $|a_1 a_2 \bar{b}_1 \bar{b}_2\rangle$ and $|\bar{a}_1 \bar{a}_2 b_1 b_2\rangle$) are degenerate with respect to the Ising Hamiltonian, and, consequently, the two corresponding diagonal elements of the HDVV Hamiltonian are also identical. Therefore, they can be combined, and one of the combinations recovers the symmetry of one of the three spin states, the triplet one. The absence of symmetry in the heterodinuclear complexes breaks this degeneracy, and it is not possible to combine BS solutions to reconstruct a spin state. Nevertheless, an appropriate mapping can be found as previously described and illustrated in Figure 1.

5. COMPUTATIONAL DETAILS

Explicitly correlated wave function and DFT methods have been used to obtain the appropriate energy values to be used in the corresponding mapping. In the first case, we used a variety of methods of increasing accuracy, starting with the CASSCF wave function³¹ as a reference to second-order perturbation, introduced through the well-known CASPT2^{32–34} procedure, and to variational multireference configuration interaction (MRCI) calculations using the difference dedicated configuration interaction (DDCI)³⁵ method. To complete the study, a series of hybrid DFT calculations have been carried out to extract the magnetic coupling constants with state-of-the-art exchange-correlation functionals. A number of such exchange-correlation potentials have been used, starting with the popular B3LYP hybrid,^{36,37} the BHHLYP (or BHandHLYP)³⁸ one, and including the M06 and M06-2X meta hybrid functionals of Zhao and Truhlar^{39–41} and the short-range HSE⁴² and long-range LC- ω PBE⁴³ range-separated functionals with the standard value of the range separation parameter (ω). Note that the selected functionals incorporate different amounts of Fock exchange: 20% for B3LYP, 27% for M06, 50% for BHandHLYP, and 54% for M06-2X. In all cases, the DFT calculations were carried out within the spin-polarized (unrestricted) formalism based on a single determinant, and high spin and BS solutions were considered. In order to avoid the problems encountered when dealing with BS solutions, calculations have also been carried out with the time-dependent DFT (TDDFT)^{44–47} in its spin flip variant.^{48–50} Previous work on Cu dinuclear complexes²⁷ has shown that, for a given

functional, spin flip TDDFT calculated magnetic coupling constants are consistent with those obtained from the appropriate mapping (spin projection). We anticipate, however, that this method encounters severe problems when aiming at obtaining the singlet–triplet and doublet–quartet splitting of the present heterodinuclear systems, thus hampering the prediction of the corresponding magnetic couplings. It is worth pointing out that some alternative methods have been proposed to calculate exchange couplings, such as the variation of constrained DFT⁵¹ based on the use of coupled-perturbed Kohn–Sham equations as proposed by Phillips and Peralta.⁵² However, to our knowledge, this method has not been used in heteronuclear systems. It would be interesting to see if it can reproduce the exchange couplings in this case, where spin flip TDDFT fails to give physical results.

The wave function and DFT calculations were carried out using suitable Gaussian-type orbitals (GTO) basis sets. For nonmetal atoms, the all electron standard 6-31G(d) basis set has been selected. For the metallic centers, we used either all electron (AE) or effective core potential (ECP) bases. In the first case, we used the rather large standard basis set GTO 6-3111+G for V, Ni, and Cu. From a technical point of view one must mention that in the calculations with the Gaussian code this basis was entered manually since otherwise the results obtained correspond actually to the 6-311G basis. For the calculations where the metal innermost electrons are described through an ECP, we used the extended standard LANL2TZ small core basis, which allows one to take scalar relativistic effects into account. The basis sets chosen were the same as in previous works^{11,53,54} except for the computationally expensive NiVO (compound 4), where the polarization functions of the light atoms basis set have been removed leading simply to a 6-31G basis set.

To make DDCI calculations feasible, we used 6-31G for C and H, 6-31G(d) for O and N, and all electron 6-3111+G for metal atoms. It was proven that there is no important deviation in doing so at CASSCF level. For compound 2 CASSCF(3,3) with 6-31G(d) yields a $J = -13.1$ (638 basis functions) and $J = -12.9$ (518 basis functions) with 6-31G for H, C. For compound 5 CASSCF(3,3) with 6-31G(d) yields $J = 30.8$ (516 basis functions) and $J = 31.4$ (421 basis functions) with 6-31G for H, C. For compound 6 CASSCF(3,3) with 6-31G(d) yields a $J = 23.4$ (678 basis functions) and $J = 23.5$ (543 basis functions) with 6-31G for H, C. More details can be found in Table S11 (Supporting Information).

For the CASSCF calculations, two types of active space were defined, a minimal one including the magnetic orbitals only and one including molecular orbitals centered on the bridging ligands. For the singlet–triplet systems this leads to a two-electron-in-two-orbitals active space (CASSCF(2,2)), whereas for the doublet–quartet systems one has a three-electron-in-three-orbitals active space (CASSCF(3,3)). The second type of active space involves CASSCF(12,12) and CASSCF(13,13) for singlet–triplet systems and for doublet–quartet systems, respectively, and were essentially carried out to verify that the minimal CAS description is physically meaningful (see Tables S1–S4 of the Supporting Information). In this respect, care was taken to ensure that all of the MOs in the active space are equivalent when using both LANL2TZ and AE 6-3111+G basis sets for the metal atoms. To avoid intruder states in the CASPT2 treatment, an imaginary level shift⁵⁵ of 0.2 au has been applied. In the most recent version of CASPT2, the zero-order Fock operator is modified with a so-called IPEA shift.⁵⁶

In the present work, and following previous research on magnetic systems,⁵⁷ this shift has been removed. Finally, to reduce the computational burden, we have applied the Cholesky decomposition to the two-electron integrals^{58,59} with the default threshold of 10^{-4} .

MRCI calculations using the difference dedicated configuration DDCI method³⁵ have been carried out, starting from minimal CASSCF as the reference state. The DDCI leads to a configuration interaction expansion which is a subset of the full MRSDCI, neglecting the 2h–2p (h = hole; p = particle) excitations involving orbitals out of the CAS, which at second order of perturbation theory equally contribute to the two states, provided the same set of molecular orbitals is used.⁶⁰ Both DDCI2 and DDCI methods, including two and three degrees of freedom for excitations out of the CAS, respectively, have been used. In the case of the doublet–quartet systems (compounds 2 and 3), the DDCI calculations have been carried out with the orbital set optimized for the quartet state. In the case of the singlet–triplet systems (compounds 5 and 6), the DDCI calculations were carried out with three different sets of orbitals, those of the singlet, triplet, and the state specific (SS) ones. The large size of the molecules studied required a reduction in the active electrons and virtual orbitals to produce tractable DDCI spaces of the order of 10^8 – 10^9 determinants. Thus, for compound 2 we explicitly treat 211 electrons in 317 orbitals; for compound 3, 238 electrons in 320 orbitals; and for compounds 5 and 6, 166 electrons in 274 orbital and 220 electrons in 338 orbitals, respectively. Additional information can be found in the Supporting Information.

All calculations were performed on the crystallographic structures of the isolated heterodimetallic complexes (cationic or neutral) in vacuo, in order to prevent mixing structural and electronic effects and avoid introducing errors in the magnetic coupling constants arising from errors in the structure optimization. For structures 1 (PAJZAB) and 2 (PAJZEF), it was necessary to previously optimize the disordered atoms ($C_3H_6NH_2$ and CH_3 moieties, respectively) together with the “lost” hydrogen atoms, using the B3LYP method on the quartet state.

The DFT based calculations have been carried out using the Gaussian 09 suite of programs.⁶¹ The electronic structure packages Q-Chem 3.2⁶² and GAMESS^{63,64} were used for the SF-TDDFT calculations. Q-Chem 3.2 allows one to use only unrestricted reference states, whereas GAMESS can employ both restricted and unrestricted reference states. MOLCAS 7.8⁶⁵ was used to perform the CASPT2 calculations. Finally, DDCI calculations were carried out using the CASDI code⁶⁶ interfaced to the MOLCAS 7.6 package⁶³ which provided the CASSCF reference wave functions.

6. RESULTS AND DISCUSSION

a. Results from CASSCF/CASPT2 Calculations. For the singlet–triplet cases, the minimal (2,2) active space was completed with molecular orbitals centered on the ligands up to a (12,12) size. It is interesting to underline the character of those orbitals. For CuVO containing compounds 5 and 6, besides the magnetic orbitals, there are two π molecular orbitals (MOs) with contribution in the oxygen atoms between the metallic centers, three MOs that form the V–O bond, and the corresponding five antibonding MOs. For the doublet–quartet cases in compounds 1–4, the minimal (3,3) active space was completed with molecular orbitals centered on the ligands up to a (13,13) size. For compounds 3 and 4, the additional MOs

Table 2. Calculated ab Initio J Values (cm^{-1}) of the Molecular Systems Studied^a

M ₁ M ₂ /compd	method					J _{exp}
	CASPT2		orbitals/CAS	DDCI		
				DDCI2	DDCI	
	LANL2	AE		AE	AE	
NiCu/1	−49.5	−45.2				−96.3
NiCu/2	−68.9	−62.3	Q/3,3	−23.5	−61.1	−117.8
NiVO/3	−15.9	−16.2	Q/3,3	−10.1	−16.8	−17.8
NiVO/4	−15.7	−15.2				−20.0
CuVO/5	71.8	65.0	T/2,2	39.9	81.1	118
			T/4,4	40.1	73.6	
			S/4,4		72.1	
			SS/4,4		83.3	
CuVO/6	55.5	49.6	T/2,2	22.6	60.4	85
			S/2,2		59.4	
			SS/2,2		66.8	

^a M_1M_2 specifies the couple of magnetic centers; LANL2 and AE stand for calculations carried out with effective core potentials or all electron, respectively. The CASPT2 calculations use the minimal (3,3) or (2,2) active space. The basis sets are as specified in the text; note that in the DDCI calculations C and H atoms are described with a standard 6-31G basis set. S, T, D, Q, or state specific (SS) indicates the orbital set used to carry out the DDCI2 and DDCI calculations.

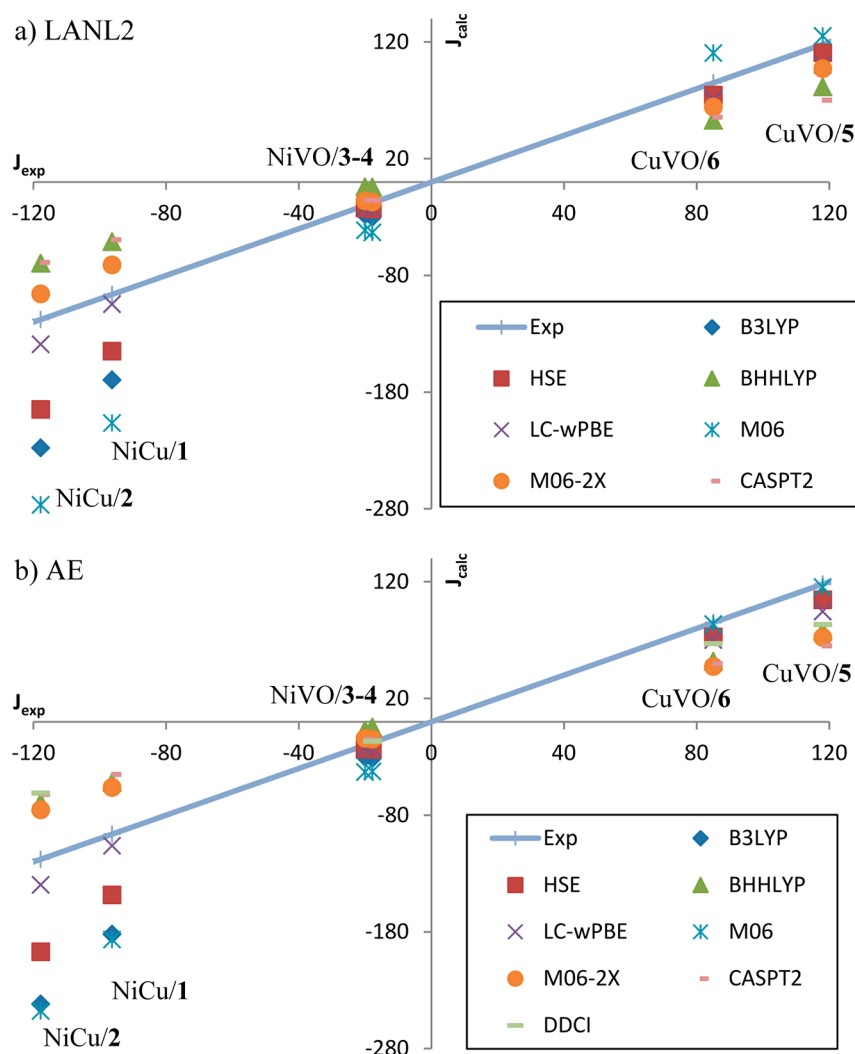


Figure 2. Schematic representation of the deviation from experiment of DFT and CASPT2 results based on the use of a broken symmetry approach, as discussed in section 6.c. The straight line indicates the perfect correlation between experimental and calculated J values (cm^{-1}) to guide the eye. Panel a presents the results using LANL2 pseudopotential for the description of the metallic center; panel b, for the all electron description including both CASPT2 and DDCI results.

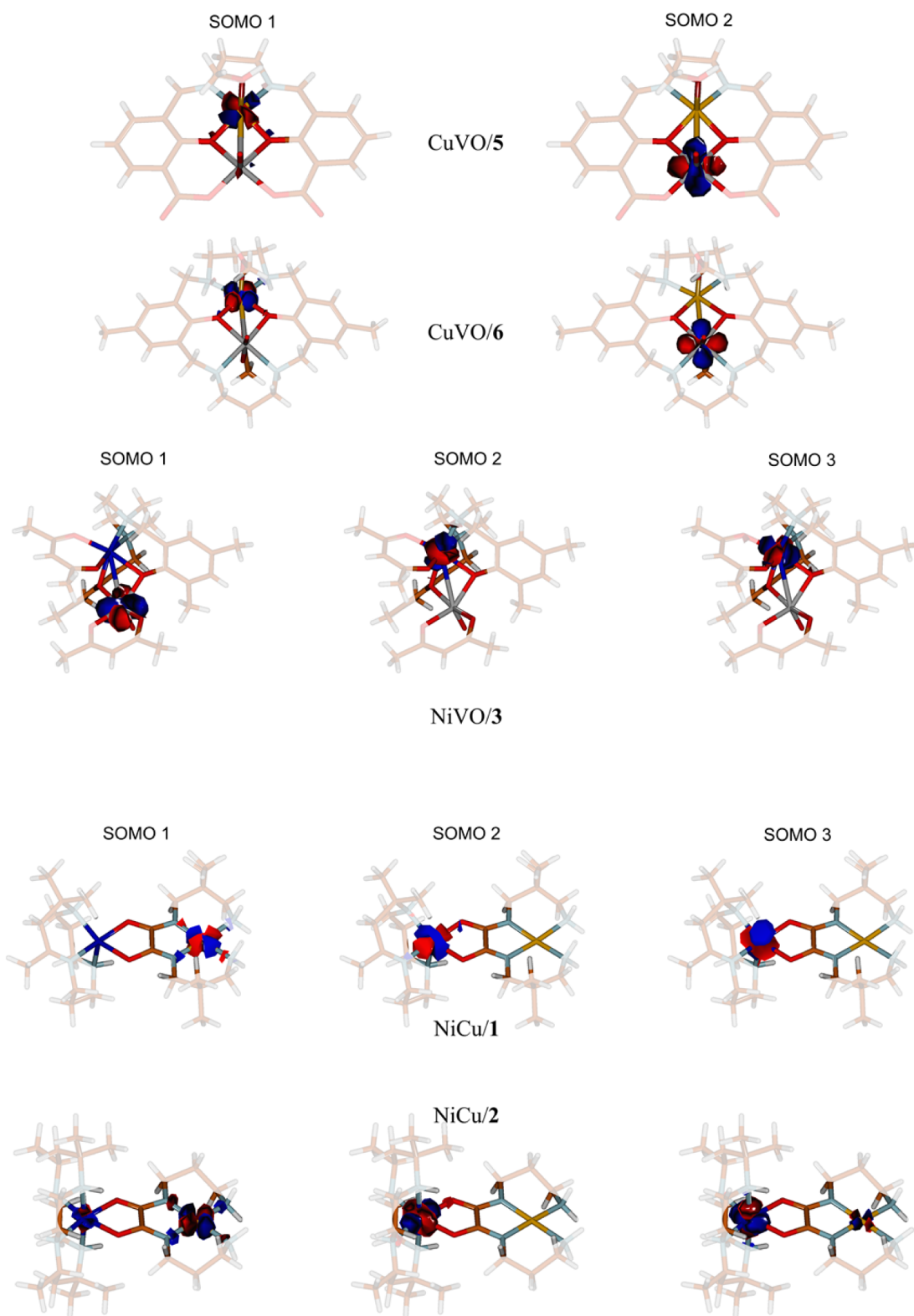


Figure 3. Contour plots of the relevant magnetic orbitals of compounds 1–3, 5, and 6 taken from the CASSCF high spin state wave function.

are completely analogous to those previously described for the CuVO systems 5 and 6, namely, three of σ type with respect to the plane of the ligands and two of π type with the correlating five antibonding MOs.

At the CASSCF level, the magnetic coupling constants calculated with the minimal and extended active spaces are almost identical indicating (Tables S1–S5 in the Supporting

Information) that the former contains the physically meaningful orbitals. Consequently, CASPT2 calculations presented in Table 2 correspond to the minimal CAS; CASPT2 calculations for the more extended CAS are presented in Table S2 of the Supporting Information. From Table 2 it is clear that, with a minimal active space, CASPT2 is only capable of providing qualitatively correct results and it underestimates the value of

the magnetic coupling for both ferromagnetic and antiferromagnetic complexes, in line with previous work.¹³ Results from CASPT2 on top of the extended CAS (Table S2 of the Supporting Information) do not improve the description indicating the need to go beyond second-order perturbation theory and justify carrying out the computationally demanding DDCI calculations described later. Overall, the calculated J values are slightly better when LANL2TZ is used for the metals, as compared with the all electron 6-3111+G basis set. Exceptions are 3 and 4, for which CASPT2 and experiment are in good agreement.

The recovery of, in general, a fraction of magnetic coupling only with CASPT2, and their underestimate, are well-known.^{55,67} An essential limitation of the method is that the computational cost rises steeply with the size of the CASSCF active space. Furthermore, both the present report and previous work have shown that CASPT2 prediction of magnetic couplings strongly depends on several technical parameters. In the version of CASPT2 we have employed, namely, the one implemented in the MOLCAS 7.8 package,⁶³ the default zero-order Hamiltonian contains the so-called IPEA shift (see Computational Methods). The purpose of this shift is to balance the description of closed and open shell systems. In the present study and following previous work,⁶⁵ we set this shift to zero. The standard value of this shift (0.25 au) gave the wrong ground state for CuVO. In the literature, widely different values of the IPEA shift have been employed, ranging from zero to 0.70 au.^{68–72} Also in CASPT2, the presence of intruder states forces one to either increase the size of the active space, which is not always possible or convenient, or to introduce a level shift. Using a value of the imaginary level shift of 0.20 au, all obtained magnetic couplings are reasonable, and we have adopted that value. However, an important uncertainty remains, namely, whether the heteronuclear systems considered can be described with the Heisenberg Hamiltonian. The present systems, with a total of two or three magnetic electrons, only produce two electronic states and an energy difference, which can always be related to a value of J . For systems such that several magnetic electronic states are possible, it has been found that CASPT2 does not fulfill the Landé interval rule,⁶⁵ as it should for a complex well-described by the Heisenberg Hamiltonian. This problem is likely to be due to the use of different orbitals for each state, as reported earlier for Fe dinuclear complexes.⁷³ The logic is that each set of orbitals spans a different effective Hamiltonian and, hence, there is no one-to-one mapping. This problem could be ignored at a pragmatic level choosing the two electronic states that give the best value of J , but of course this cannot be regarded as satisfactory at a theoretical level.

From all of the preceding discussion, one can conclude that the CASPT2 method, at least in its current form, is not suitable for the study of magnetic systems. CASPT2 can describe relatively simple systems at a qualitative level, but a quantitative prediction is not possible, since there are at present too many uncertainties for its application to general magnetic systems.

b. Results from DDCI Calculations. To further confirm that the shortcomings of the CASPT2 method arise from the neglect of important dynamical correlation effects, DDCI calculations have been carried out for those compounds where molecular size is not excessive, as reported in Table 2. A schematic representation of the results can be found in Figure 2. For the singlet–triplet systems 2 and 3, DDCI results are close to those obtained with the CASPT2 approach. For

compound 3 both methods predict results in very good agreement with experiment. However, for compound 2 both CASPT2 and DDCI results considerably underestimate the experimental magnetic coupling constant. The reason is likely to be due to the contribution of bridging ligands to the differential correlation effects. This is corroborated by the orbital contours in Figure 3 showing a considerable delocalization of the active orbitals beyond the magnetic centers. For compounds 5 and 6, DDCI represents a significant improvement over CASPT2, although the DDCI calculated magnetic coupling constants still underestimate the experimental values.

The conclusion from these very demanding calculations is that, for real systems with bulky ligands and different magnetic centers, electronic correlation effects are very important and not recovered by excitation out of the minimal CAS implying that higher excitations still play a role. Note also that some of the DDCI calculations required neglecting excitation from/to some core and virtual orbitals. Enlarging the CAS is certainly possible, but the resulting DDCI expansion is too large to be handled.

In addition one has to point out that, compared to homobimetallic systems, heterobimetallic complexes have some peculiarities. For instance, in a very recent report, several homo- and heterobimetallic complexes of divalent first-row transition metal atoms (Mn, Fe, and Co) with a direct bonding between the metals were synthesized and their properties compared.⁷⁴ All of the complexes are antiferromagnetic, but the di-iron complex is different from the rest in that it contains a metal–metal single bond and a septet ground state. In contrast, the other complexes have weak metal–metal interactions and much lower spin states. Also, in recent reports it has been shown that heterobimetallic systems in their singlet states have particularly large values of second hyperpolarizabilities, in turn giving rise to large third-order nonlinear optical (NLO) effects. This finding has been attributed to the contribution of electrons with an intermediate diradical character, and it is more marked in heterobimetallic systems due to charge asymmetry effects.^{75,76}

c. Results from Spin Flip TDDFT Calculations. To test the performance of the SF-TDDFT method, calculations were carried out for the M06, BHHLYP, and M06-2X functionals only. For the singlet–triplet cases, an approximately correct spin state is obtained with the BHHLYP functional. For the CuVO complex 5, using the LANL2DZ basis functions for the metallic ions and an unrestricted reference, we obtain $\langle \hat{S}^2 \rangle = 1.96$ and 0.13 for the approximate triplet and singlet states, respectively. The predicted magnetic coupling of $J = 81 \text{ cm}^{-1}$ is in agreement with the BS results presented later using the same functional but too small compared to experiment. Moreover, for the CuVO complex 6, using the all electron basis sets for the metals and an unrestricted reference, we obtain $\langle \hat{S}^2 \rangle = 1.86$ and 0.29, and a magnetic coupling of $J = 65 \text{ cm}^{-1}$. Interestingly, better spin adaptation is obtained with unrestricted references as compared to restricted references. So far, results are in agreement with previous work in homodinuclear compounds.²⁷

The situation is completely different for the doublet–quartet cases. In fact, for compounds 3 and 4, we obtain values of $\langle \hat{S}^2 \rangle$ very far from the expected values of 0.75 and 3.75 for the doublet and quartet, respectively. Thus, the obtained values of $\langle \hat{S}^2 \rangle$ are 1.75 and 2.75 for the lowest two spin flip states. Note

that the expectation value for the doublet corresponds to the SBS, as defined in section 4.b, which is clear evidence that the spin flip approach for the doublet state actually describes a mixture of doublet and quartet states. As a consequence, in these cases it is not possible to estimate the values of magnetic coupling from SF-TDDFT, at least with the current implementations where all excitations are allowed.

The reason for the large deviation is the presence of single excitations that destroy the high spin coupling in the Ni atom, thus mixing local singlet and triplet states. In conclusion, SE-TDDFT is not capable of providing a uniformly correct description of the six heteronuclear complexes studied. Whereas an approximately correct spin adaptation and good values of J are obtained for the singlet–triplet cases, for the doublet–quartet cases the values of $\langle \hat{S}^2 \rangle$ and the magnetic couplings are far from the experiment even in the most favorable cases. Apparently, whether one obtains well-spin-adapted solutions depends very sensitively on the density functional and on its percentage of exact exchange. This is in contrast to the case of homonuclear complexes, where good results can be obtained with a single density functional for a range of complexes.^{27,77}

d. Results from DFT Calculations with the BS Approach. The last inspection concerns the monodeterminantal description of the compounds by means of broken symmetry approach. Taking into account the problematic discussed in section 4.b. results are summarized in Table 3 and schematically depicted in Figure 2. Additional information regarding for instance $\langle \hat{S}^2 \rangle$ values can be found in the Supporting Information (Tables S5–S10).

A first thing to notice is the strong dependence on the chosen functional. Taking compound **1** as an example, the deviation with respect to the experimental value ranges from +94% for the M06 and B3LYP functionals to -46% for BHHLYP. The dependence in the functional can also be observed in Tables 4 and 5 reporting the spin density on the metallic centers as predicted by the DFT methods used although a correlation between the trends in calculated J values and spin densities does not seem to exist. The tables report results from the all electron series of calculations although very similar values are obtained when describing the core electrons by ECPs. Among all of the functionals, the long-range corrected LC- ω PBE potential comparatively gives the best results for all compounds. Among the compounds, as depicted in Figure 2, there are two families: the ferromagnetic one where the energetic difference is between singlet-triplet states (CuVO/5-6) and the antiferromagnetic one presenting compounds with a doublet electronic state as ground state (NiCu/1-2, NiVO/3-4). There is a general underestimation of the coupling constant in the first family while the opposite stands for the antiferromagnetic compounds. Compounds **1** and **2** are poorly described by the majority of functionals, presenting the biggest deviations in the case of the B3LYP, HSE, and M06 hybrid functionals, as represented in the leftmost values in Figure 2. The reason behind the different agreement with respect to experimental values for compounds **1-2** and **3-4** might be the large difference in distance between the two metallic centers and the different chemical nature of the bridge, the π system of the oxamato bridge in **1-2** as opposed to the μ -O bridges in **3-4** (see Figure 3).

Moreover, for the M06 and M06-2X hybrid functionals there is a considerable impact depending on how the metallic center

Table 3. Calculated DFT J Values (cm^{-1}) of the Molecular Systems Studied Using the Broken Symmetry Approach^a

M ₁ M ₂ /compd	method												$J_{\text{exp}}/\text{cm}^{-1}$
	B3LYP		HSE		BHHLYP		LC- ω PBE		M06		M06-2X		
	LANL2	AE	LANL2	AE	LANL2	AE	LANL2	AE	LANL2	AE	LANL2	AE	
NiCu/1	-169.50	-182.01	-144.86	-148.03	-51.17	-52.06	-104.52	-106.16	-206.42	-186.50	-70.97	-56.21	-96.3
NiCu/2	-227.74	-241.78	-194.89	-197.07	-69.53	-69.29	-138.97	-139.67	-276.62	-247.71	-95.82	-75.41	-117.8
NiVO /3	-30.1	-31.3	-23.1	-23.6	-4.4	-4.6	-22.3	-22.7	-43.1	-42.5	-17.1	-14.9	-17.8
NiVO /4	-27.9	-30.2	-22.3	-23.3	-4.2	-7.3	-21.8	-22.5	-41.3	-43.0	-16.0	-14.2	-20.0
CuVO /5	+108.0	+106.6	+110.8	+104.5	+81.5	+77.6	+100.3	+94.5	+125.2	+115.4	+97.2	+72.4	118
CuVO /6	+74.3	+75.6	+74.5	+72.7	+52.8	+51.9	+71.0	+70.0	+110.6	+83.8	+64.4	+47.4	85

⁷LANL2 and AE stand for calculation with effective core potentials and all electron, respectively.

Table 4. Spin Density on the Metallic Centers of NiCu Compounds 1 and 2 As Predicted by the Different Computational Methods Used with the Broken Symmetry Approach^a

method	compd 1				compd 2			
	Ni(II)		Cu (II)		Ni(II)		Cu(II)	
	HS	BS	HS	BS	HS	BS	HS	BS
BHandHLYP	1.81	1.81	0.75	−0.75	1.81	1.81	0.74	−0.74
B3LYP	1.67	1.67	0.60	−0.60	1.67	1.67	0.60	−0.59
HSEh1PBE	1.71	1.71	0.63	−0.63	1.71	1.71	0.62	−0.62
LC- ω PBE	1.71	1.71	0.64	−0.64	1.71	1.71	0.63	−0.63
M06	1.69	1.68	0.61	−0.61	1.69	1.69	0.60	−0.60
M062x	1.80	1.80	0.76	−0.75	1.80	1.80	0.75	−0.75

^aReported values correspond to the series of all electron calculations. HS and BS stand for the high spin and broken symmetry solutions, respectively.

Table 5. Spin Density on the Metallic Centers of NiVO Compounds 3 and 4 and CuVO Compounds 5 and 6 As Predicted by the Different Computational Methods Used with the Broken Symmetry Approach^a

method	compd 3				compd 4				compd 5				compd 6			
	VO(II)		Ni(II)		VO(II)		Ni(II)		VO(II)		Cu(II)		VO(II)		Cu(II)	
	HS	BS	HS	BS	HS	BS	HS	BS	HS	BS	HS	BS	HS	BS	HS	BS
BHandHLYP	1.22	−1.23	1.82	1.82	1.22	−1.22	1.82	1.81	1.17	−1.17	0.79	0.79	1.31	1.31	0.84	−0.84
B3LYP	1.13	−1.13	1.69	1.67	1.12	−1.13	1.69	1.68	1.09	−1.08	0.65	0.65	1.18	1.18	0.70	−0.70
HSEh1PBE	1.16	−1.16	1.72	1.72	1.15	−1.15	1.72	1.72	1.11	−1.11	0.68	0.68	1.22	1.22	0.73	−0.73
LC- ω PBE	1.16	−1.16	1.73	1.72	1.15	−1.16	1.72	1.72	1.11	−1.11	0.69	0.69	1.22	1.22	0.74	−0.74
M06	1.24	−1.24	1.71	1.70	1.23	−1.24	1.70	1.70	1.18	−1.17	0.66	0.66	1.32	1.32	0.71	−0.71
M062x	1.21	−1.21	1.81	1.80	1.21	−1.21	1.81	1.80	1.16	−1.16	0.79	0.79	1.28	1.28	0.83	−0.84

^aReported values correspond to the series of all electron calculations. HS and BS stand for the high spin and broken symmetry solutions, respectively.

is described, i.e., using an effective core potential or an all electron basis set. This is not observed for the rest of the methods, as indicated by Figure 2. As previously reported,⁵² this is an indication of a pathology present in these functionals. It could also be argued that the ECPs obtained through the Hartree–Fock formalism are not appropriate to describe the M06 cores although this remains to be proven.

7. CONCLUSION

In this work we have investigated magnetic coupling in several heterodinuclear complexes by means of a variety of DFT and wave function based methods. In each case, appropriate mappings are presented enabling one to extract the magnetic coupling constant from total energy differences, provided the correct solutions are used. This is a particularly delicate issue when using DFT based methods within the BS approach. In fact, the current implementation of spin flip DFT appears to be useless in the case of NiCu and NiVO compounds since the excitations involved break the local triplet in Ni resulting in severe spin contamination thus hindering the use of mapping approaches. On the other hand, the use of a broken symmetry approach requires careful analysis, especially in the case of doublet states. This is because, in this case, it is not possible to define a spin projector allowing one to reconstruct the pure doublet state from the BS solutions. However, a mapping procedure using the expectation values of the Heisenberg Hamiltonian with an appropriate BS determinant provides a consistent relationship to derive J values from BS solutions. Note, however, that obtaining corresponding solutions with the appropriate d orbital occupancy is not always straightforward.

Regarding the predicted values, a large dispersion of the calculated results exists. Apart from the well-known depend-

ence of the calculated results with respect to the exchange-correlation functional,¹² the DFT based methods tend to overestimate (in absolute value) antiferromagnetic interactions and to underestimate ferromagnetic ones. Nevertheless, qualitative values are obtained and regular trends are always observed. Interestingly, the best results are obtained with LC- ω PBE functional, in agreement with previous work for Cu-dinuclear complexes,^{51,78} and the worst correspond to M06 and B3LYP methods. Note, however, the LC- ω PBE does not perform so well in organic diradical whereas the opposite holds for M06 and, especially, M06-2X.⁷⁹

The explicitly correlated CASPT2 and DDCI wave function based methods show accuracy similar to the best DFT approach although both tend to underestimate (in absolute value) antiferromagnetic and ferromagnetic interactions. This is, in part, related to the use of minimal CAS containing the magnetic orbitals only. Nevertheless, DDCI and CASPT2 results show a balanced behavior over the whole range of J values.

Compounds 3 and 4 containing the NiVO magnetic centers are homogeneously well described by most of the methods whereas, despite belonging to the antiferromagnetic family with quartet–doublet magnetic states, compounds 1 and 2 containing NiCu present the largest deviations and dispersion. The differential behavior in these four compounds can be ascribed to the different nature of the ligands bridging the metallic centers. Compounds 5 and 6 are both ferromagnetic, the magnetic coupling constant, involving a singlet–triplet energy difference, is homogeneously described by all of the methods, although always underestimated.

To summarize, magnetic coupling in heteronuclear complexes can be predicted from accurate total energy differences.

In the case of using wave function based methods the procedure and the performance is as in other dinuclear complexes. However, when using DFT based methods, the lack of left–right symmetry in the metallic center has important consequences and special care is needed on selecting the appropriate broken symmetry solutions and on using the appropriate mapping.

■ ASSOCIATED CONTENT

■ Supporting Information

Tables listing energies and coupling constants for triplet/singlet cases, Mulliken spin densities on the transition metal atoms, and details about the number of electrons. This material is available free of charge via the Internet at <http://pubs.acs.org>.

■ AUTHOR INFORMATION

Corresponding Author

*E-mail: francesc.illas@ub.edu.

Notes

The authors declare no competing financial interest.

■ ACKNOWLEDGMENTS

This work has been supported by Spanish MICINN through Research Grants PRI-PIBIN-2011-1028 and CTQ2012-30751 and by Generalitat de Catalunya Grants 2014SGR97 and XRQTC. F.I. acknowledges additional financial support through the 2009 ICREA Academia Award for Excellence in University Research.

■ REFERENCES

- (1) Caneschi, A.; Gatteschi, D.; Sessoli, R.; Rey, P. Toward Molecular Magnets—The Metal–Radical Approach. *Acc. Chem. Res.* **1989**, *22*, 392–398.
- (2) Christou, G.; Gatteschi, D.; Hendrickson, D. N.; Sessoli, R. Single-Molecule Magnets. *MRS Bull.* **2000**, *25*, 66–71.
- (3) Alivisatos, A. P.; Barbara, P. F.; Castleman, A. W.; Chang, J.; Dixon, D. A.; Klein, M. L.; McLendon, G. L.; Miller, J. S.; Ratner, M. A.; Rossky, P. J.; Stupp, S. I.; Thompson, M. E. From molecules to materials: Current trends and future directions. *Adv. Mater.* **1998**, *10*, 1297–1336.
- (4) Ribas, J.; Escuer, A.; Monfort, M.; Vicente, R.; Cortes, R.; Lezama, L.; Rojo, T. Polynuclear Ni-II and Mn-II Azido Bridging Complexes. Structural Trends and Magnetic Behavior. *Coord. Chem. Rev.* **1999**, *193–195*, 1027–1068.
- (5) Milios, C. J.; Inglis, R.; Vinslava, A.; Bagai, R.; Wernsdorfer, W.; Parsons, S.; Perlepes, S. P.; Christou, G.; Brechin, E. K. Toward a Magnetostructural Correlation for a Family of Mn_6 SMMs. *J. Am. Chem. Soc.* **2007**, *129*, 12505–12511.
- (6) Gatteschi, D.; Sessoli, R. Quantum Tunneling of Magnetization and Related Phenomena in Molecular Materials. *Angew. Chem., Int. Ed.* **2003**, *42*, 268–297.
- (7) A general review of the different classes of molecular magnetic materials is provided in the “molecule-based magnets” special issue of *MRS Bull.* **2000**, *25* (11).
- (8) Rajca, A. Organic Diradicals and Polyradicals: From Spin Coupling to Magnetism? *Chem. Rev.* **1994**, *94*, 871–893.
- (9) Iwamura, H.; Koga, N. Studies of Organic Di-, Oligo-, and Polyradicals by Means of Their Bulk Magnetic Properties. *Acc. Chem. Res.* **1993**, *26*, 346–351.
- (10) Ruiz, E.; Alemany, P.; Alvarez, S.; Cano, J. Toward the Prediction of Magnetic Coupling in Molecular Systems: Hydroxo- and Alkoxo-Bridged Cu(II) Binuclear Complexes. *J. Am. Chem. Soc.* **1997**, *119*, 1297–1303.
- (11) Valero, R.; Costa, R.; Moreira, I. de P. R.; Truhlar, D. G.; Illas, F. Performance of the M06 Family of Exchange-Correlation Functionals

for Predicting Magnetic Coupling in Organic and Inorganic Molecules. *J. Chem. Phys.* **2008**, *128*, No. 114103.

(12) Moreira, I. de P. R.; Illas, F. A Unified View of the Theoretical Description of Magnetic Coupling in Molecular Chemistry and Solid State Physics. *Phys. Chem. Chem. Phys.* **2006**, *8*, 1645–1659.

(13) Malrieu, J. P.; Caballol, R.; Calzado, C. J.; de Graaf, C.; Guihéry, N. Magnetic Interactions in Molecules and Highly Correlated Materials: Physical Content, Analytical Derivation, and Rigorous Extraction of Magnetic Hamiltonians. *Chem. Rev.* **2014**, *114*, 429–492.

(14) Caballol, R.; Castell, O.; Illas, F.; Malrieu, J. P.; Moreira, I. de P. R. Remarks on the Proper Use of the Broken Symmetry Approach to Magnetic Coupling. *J. Phys. Chem. A* **1997**, *101*, 7860–7866.

(15) Illas, F.; Moreira, I. de P. R.; de Graaf, C.; Barone, V. Magnetic Coupling in Biradicals, Binuclear Complexes and Wide Gap Insulators: A Survey of Ab Initio Wave Function and Density Functional Theory Approaches. *Theor. Chem. Acc.* **2000**, *104*, 265–272.

(16) Neese, F. Prediction of Molecular Properties and Molecular Spectroscopy with Density Functional Theory: From Fundamental Theory to Exchange-Coupling. *Coord. Chem. Rev.* **2009**, *253*, 526–563.

(17) de Jongh, L. J.; Miedema, A. R. Experiments on Simple Magnetic Model Systems. *Adv. Phys.* **2001**, *50*, 947–1170 (Reprinted from *Advances in Physics*, Vol. 23, 1974).

(18) Mattis, D. C. *The Theory of Magnetism*, Springer Series in Solid-State Sciences, Vols. 17 and 55; Springer-Verlag: Berlin, 1985.

(19) Yosida, K. *Theory of Magnetism*, Springer Series in Solid-State Sciences, Vol. 122; Springer-Verlag, Berlin, 1996.

(20) Moreira, I. de P. R.; Illas, F.; Calzado, C. J.; Sanz, J. F.; Malrieu, J. P.; Ben Amor, N.; Maynau, D. Local Character of Magnetic Coupling in Ionic Solids. *Phys. Rev. B* **1999**, *59*, R6593–R6596.

(21) Muñoz, D.; Moreira, I. de P. R.; Illas, F. Accurate Prediction of Large Antiferromagnetic Interactions in High-T_c $HgBa_2Ca_{n-1}Cu_nO_{2n+2+\delta}$ ($n=2,3$) Superconductor Parent Compounds. *Phys. Rev. Lett.* **2000**, *84*, 1579–1582.

(22) Fink, K.; Wang, C.; Staemmler, V. Superexchange and Spin–Orbit Coupling in Chlorine-Bridged Binuclear Cobalt(II) Complexes. *Inorg. Chem.* **1999**, *38*, 3847–3856.

(23) Escuer, A.; Vicente, R.; Ribas, J.; Costa, R.; Solans, X. New Nickel(II)–Copper(II) Heterodinuclear Complexes with Hexa- and Pentacoordinated Nickel(II) Ions. Magnetostructural Correlations. *Inorg. Chem.* **1992**, *31*, 2627–2633.

(24) Mandal, D.; Chatterjee, B. P.; Ganguly, R.; Tiekink, E. R. T.; Clérac, R.; Chaudhury, M. Tetra- and Dinuclear Nickel(II)–Vanadium(IV/V) Heterometal Complexes of a Phenol-Based N_2O_2 Ligand: Synthesis, Structures, and Magnetic and Redox Properties. *Inorg. Chem.* **2008**, *47*, 584–591.

(25) Kahn, O.; Galy, J.; Journaux, Y.; Jaud, J.; Morgenstern-Badaraui, I. Synthesis, Crystal Structure and Molecular Conformations, and Magnetic Properties of a Copper–Vanadyl (CuII–VOII) Heterobinuclear Complex: Interaction between Orthogonal Magnetic Orbitals. *J. Am. Chem. Soc.* **1982**, *104*, 2165–2176.

(26) Mohanta, S.; Nanda, K. K.; Thompson, L. K.; Flörke, U.; Nag, K. Spin Exchange Coupling in Heterobimetallic $M^{II}V^{IV}O$ ($M = Cu, Ni, Co, Fe, Mn$) Macrocyclic Complexes. Synthesis, Structure, and Properties. *Inorg. Chem.* **1998**, *37*, 1465–1472.

(27) Valero, R.; Illas, F.; Truhlar, D. G. Magnetic Coupling in Transition Metal Binuclear Complexes by Spin-Flip Time-Dependent Density Functional Theory. *J. Chem. Theory Comput.* **2011**, *7*, 3523–3531.

(28) Yamaguchi, K.; Takahara, Y.; Fueno, T.; Nasu, K. Ab Initio MO Calculations of Effective Exchange Integrals between Transition-Metal Ions via Oxygen Dianions: Nature of the Copper–Oxygen Bonds and Superconductivity. *Jpn. J. Appl. Phys.* **1987**, *26*, No. L1362.

(29) Yamaguchi, K.; Jensen, F.; Dorigo, A.; Houk, K. N. A Spin Correction Procedure for Unrestricted Hartree-Fock and Møller-Plesset Wave Functions for Singlet Diradicals and Polyradicals. *Chem. Phys. Lett.* **1988**, *149*, 537–542.

(30) Yamaguchi, K.; Takahara, Y.; Fueno, T.; Houk, K. N. Extended Hartree-Fock (EHF) Theory of Chemical-Reactions 3. Projected Møller-Plesset (PMP) Perturbation Wavefunctions for Transition

Structures of Organic-Reactions. *Theoret. Chim. Acta* **1988**, *73*, 337–364.

(31) Roos, B. O.; Taylor, P. R.; Siegbahn, P. E. M. A complete active space SCF method (CASSCF) using a density matrix formulated super-CI approach. *Chem. Phys.* **1980**, *48*, 157–173.

(32) Andersson, K.; Malmqvist, P.-Å.; Roos, B. O.; Sadlej, A. J.; Wolinski, K. Second-Order Perturbation Theory with a CASSCF Reference Function. *J. Phys. Chem.* **1990**, *94*, 5483–5488.

(33) Andersson, K.; Malmqvist, P.-Å.; Roos, B. O. Second-order perturbation theory with a complete active space self-consistent field reference function. *J. Chem. Phys.* **1992**, *96*, 1218–1226.

(34) de Graaf, C.; Sousa, C.; Moreira, I.; de, P. R.; Illas, F. Multiconfigurational Perturbation Theory: An Efficient Tool to Predict Magnetic Coupling Parameters in Biradicals, Molecular Complexes, and Ionic Insulators. *J. Phys. Chem. A* **2001**, *105*, 11371–11378.

(35) Miralles, J.; Castell, O.; Caballol, R.; Malrieu, J. P. Specific CI Calculation of Energy Differences: Transition Energies and Bond Energies. *Chem. Phys.* **1993**, *172*, 33–43.

(36) Becke, A. D. Density-Functional Thermochemistry. III. The Role of Exact Exchange. *J. Chem. Phys.* **1993**, *98*, 5648–5652.

(37) Stephens, P. J.; Devlin, F. J.; Chabalowski, C. F.; Frisch, M. J. Ab Initio Calculation of Vibrational Absorption and Circular Dichroism Spectra Using Density Functional Force Fields. *J. Phys. Chem.* **1994**, *98*, 11623–11627.

(38) Becke, A. D. A New Mixing of Hartree–Fock and Local Density-Functional Theories. *J. Chem. Phys.* **1993**, *98*, No. 1372.

(39) Zhao, Y.; Truhlar, D. G. A New Local Density Functional for Main-Group Thermochemistry, Transition Metal Bonding, Thermochemical Kinetics, and Noncovalent Interactions. *J. Chem. Phys.* **2006**, *125*, 194101–194118.

(40) Zhao, Y.; Truhlar, D. G. Density Functional for Spectroscopy: No Long-Range Self-Interaction Error, Good Performance for Rydberg and Charge-Transfer States, and Better Performance on Average than B3LYP for Ground States. *J. Phys. Chem. A* **2006**, *110*, 13126–13130.

(41) Zhao, Y.; Truhlar, D. G. The M06 Suite of Density Functionals for Main Group Thermochemistry, Thermochemical Kinetics, Noncovalent Interactions, Excited States, and Transition Elements: Two New Functionals and Systematic Testing of Four M06-Class Functionals and 12 Other Functionals. *Theor. Chem. Acc.* **2008**, *120*, 215–241.

(42) Heyd, J.; Scuseria, G. E.; Ernzerhof, M. Hybrid Functionals Based on a Screened Coulomb Potential. *J. Chem. Phys.* **2003**, *518*, No. 8207; Erratum: “Hybrid Functionals Based on a Screened Coulomb Potential”. **2006**, *124*, No. 219906(E).

(43) Vydrov, O. A.; Scuseria, G. E. Assessment of a Long-Range Corrected Hybrid Functional. *J. Chem. Phys.* **2006**, *125*, 234109–234119.

(44) Runge, E.; Gross, E. K. U. Density-Functional Theory for Time-Dependent Systems. *Phys. Rev. Lett.* **1984**, *52*, 997–1000.

(45) Casida, M. E. In *Time-Dependent Density-Functional Response Theory for Molecules*; Chong, D. P., Ed.; World Scientific: Singapore, 1995; Vol. 1, pp 155–192.

(46) Bauernschmitt, R.; Ahlrichs, R. Treatment of Electronic Excitations within the Adiabatic Approximation of Time Dependent Density Functional Theory. *Chem. Phys. Lett.* **1996**, *256*, 454–464.

(47) Stratmann, R. E.; Scuseria, G. E.; Frisch, M. J. An Efficient Implementation of Time-Dependent Density-Functional Theory for the Calculation of Excitation Energies of Large Molecules. *J. Chem. Phys.* **1998**, *109*, 8218–8224.

(48) Shao, Y.; Head-Gordon, M.; Krylov, A. I. The Spin–Flip Approach within Time-Dependent Density Functional Theory: Theory and Applications to Diradicals. *J. Chem. Phys.* **2003**, *118*, 4807–4818.

(49) Hirata, S.; Head-Gordon, M. Time-Dependent Density Functional Theory within the Tamm–Dancoff Approximation. *Chem. Phys. Lett.* **1999**, *314*, 291–299.

(50) Zhekova, H.; Seth, M.; Ziegler, T. Introduction of a New Theory for the Calculation of Magnetic Coupling Based on Spin–Flip Constricted Variational Density Functional Theory. Application to Trinuclear Copper Complexes which Model the Native Intermediate in Multicopper Oxidases. *J. Chem. Theory Comput.* **2011**, *7*, 1858–1866.

(51) Rudra, I.; Wu, Q.; van Voorhis, T. Accurate magnetic exchange couplings in transition-metal complexes from constrained density-functional theory. *J. Chem. Phys.* **2006**, *124*, No. 024106.

(52) Phillips, J. J.; Peralta, J. E. Magnetic exchange couplings from constrained density functional theory: An efficient approach utilizing analytic derivatives. *J. Chem. Phys.* **2011**, *135*, No. 084108.

(53) Costa, R.; Moreira, I. de P. R.; Youngme, S.; Siri Wong, K.; Wannarit, N.; Illas, F. Towards the Design of Ferromagnetic Molecular Complexes: Magnetostructural Correlations in Ferromagnetic Triply-Bridged Dinuclear Cu(II) Compounds Containing Carboxylato and Hydroxo Bridges. *Inorg. Chem.* **2010**, *49*, 285–294.

(54) Wannarit, N.; Pakawatchai, Ch.; Mutikainen, I.; Costa, R.; Moreira, I. de P. R.; Youngme, S.; Illas, F. Hetero Triply-Bridged Dinuclear Copper(II) Compounds with Ferromagnetic Coupling: A Challenge for Current Density Functionals. *Phys. Chem. Chem. Phys.* **2013**, *15*, 1966–1975.

(55) Forsberg, N.; Malmqvist, P.-Å. Multiconfiguration Perturbation Theory with Imaginary Level Shift. *Chem. Phys. Lett.* **1997**, *274*, 196–204.

(56) Ghigo, G.; Roos, B. O.; Malmqvist, P.-Å. A Modified Definition of the Zeroth-Order Hamiltonian in Multiconfigurational Perturbation Theory (CASPT2). *Chem. Phys. Lett.* **2004**, *396*, 142–149.

(57) Queral, N.; Taratiel, D.; de Graaf, C.; Caballol, R.; Cimraglia, R.; Angeli, C. On the Applicability of Multireference Second-Order Perturbation Theory to Study Weak Magnetic Coupling in Molecular Complexes. *J. Comput. Chem.* **2008**, *29*, 994–1003.

(58) Koch, H.; Sánchez de Merás, A. M. J.; Pedersen, T. B. Reduced Scaling in Electronic Structure Calculations using Cholesky Decompositions. *J. Chem. Phys.* **2003**, *118*, 9481–9484.

(59) Pedersen, T. B.; Sánchez de Merás, A. M. J.; Koch, H. Polarizability and Optical Rotation Calculated from the Approximate Coupled Cluster Singles and Doubles CC2 Linear Response Theory Using Cholesky Decompositions. *J. Chem. Phys.* **2004**, *120*, 8887–8897.

(60) Malrieu, J. P. Cancellations Occurring in the Calculation of Transition Energies by a Perturbation Development of Configuration Interaction Matrices. *J. Chem. Phys.* **1967**, *47* (11), 4555.

(61) Frisch, M. J.; Trucks, G. W.; et al. *Gaussian 09*, Revision A.1; Gaussian: Wallingford, CT, USA, 2009.

(62) Shao, Y.; Fusti-Molnar, L.; et al. Advances in Methods and Algorithms in a Modern Quantum Chemistry Program Package. *Phys. Chem. Chem. Phys.* **2006**, *8*, 3172–3191.

(63) Schmidt, M. W.; Baldridge, K. K.; Boatz, J. A.; Elbert, S. T.; Gordon, M. S.; Jensen, J. H.; Koseki, S.; Matsunaga, N.; Nguyen, K. A.; Su, S. J.; Windus, T. L.; Dupuis, M.; Montgomery, J. A., Jr. General Atomic and Molecular Electronic Structure System. *J. Comput. Chem.* **1993**, *14*, 1347–1363.

(64) Gordon, M. S.; Schmidt, M. W. In *Theory and Applications of Computational Chemistry: The First Forty Years*; Dykstra, C. E., Frenking, G., Kim, K. S., Scuseria, G. E., Eds.; Elsevier: Amsterdam, The Netherlands, 2005; Chapter 41, pp 1167–1189.

(65) Aquilante, F.; De Vico, L.; Ferré, N.; Ghigo, G.; Malmqvist, P.-Å.; Neogrady, P.; Pedersen, T. B.; Pitonák, M.; Reiher, M.; Roos, B. O.; Serrano-Andrés, L.; Urban, M.; Veryazov, V.; Lindh, R. MOLCAS 7: The Next Generation. *J. Comput. Chem.* **2010**, *31*, 224–247.

(66) Ben Amor, N.; Maynaud, D. Size-Consistent Self-Consistent Configuration Interaction from a Complete Active Space. *Chem. Phys. Lett.* **1998**, *286*, 211–220 (CASDI program: Package developed at the Laboratoire de Chimie et Physique Quantiques, Université Paul Sabatier, Toulouse (France)).

(67) Negodaev, I.; de Graaf, C.; Caballol, R.; Lukov, V. V. On the Magnetic Coupling in Asymmetric Bridged Cu(II) Dinuclear

Complexes: The Influence of Substitutions on the Carboxylato Group. *Inorg. Chim. Acta* **2011**, 375, 166–172.

(68) Kepenekian, M.; Robert, V.; Le Guennic, B. What Zeroth-Order Hamiltonian for CASPT2 Adiabatic Energetics of Fe(II)N₆ Architectures? *J. Chem. Phys.* **2009**, 131 (114702), 1–8.

(69) Vancoillie, S.; Rulišek, L.; Neese, F.; Pierloot, K. Theoretical Description of the Structure and Magnetic Properties of Nitroxide–Cu(II)–Nitroxide Spin Triads by Means of Multiconfigurational ab Initio Calculations. *J. Phys. Chem. A* **2009**, 113, 6149–6157.

(70) Bonnet, M.-L.; Robert, V.; Tsuchiizu, M.; Omori, Y.; Suzumura, Y. Intramolecular Charge Ordering in the Multi Molecular Orbital System (TTM-TTP)I₃. *J. Chem. Phys.* **2010**, 132 (214705), 1–6.

(71) Ma, Y.; Bandeira, N. A. G.; Robert, V.; Gao, E.-Q. Experimental and Theoretical Studies on the Magnetic Properties of Manganese(II) Compounds with Mixed Isocyanate and Carboxylate Bridges. *Chem.—Eur. J.* **2011**, 17, 1988–1998.

(72) Daku, L. M. L.; Aquilante, F.; Robinson, T. W.; Hauser, A. Accurate Spin-State Energetics of Transition Metal Complexes. 1. CCSD(T), CASPT2, and DFT Study of [M(NCH)₆]²⁺ (M = Fe, Co). *J. Chem. Theory Comput.* **2012**, 8, 4216–4231.

(73) Mödl, M.; Povill, A.; Rubio, J.; Illas, F. Ab Initio Study of the Magnetic Coupling in Na₆Fe₂S₆. *J. Phys. Chem. A* **1997**, 101, 1526–1531.

(74) Tereniak, S. J.; Carlson, L. K.; Clouston, L. J.; Young, V. G., Jr.; Bill, E.; Maurice, R.; Chen, Y.-S.; Kim, H. J.; Gagliardi, L.; Lu, C. C. Role of the Metal in the Bonding and Properties of Bimetallic Complexes Involving Manganese, Iron, and Cobalt. *J. Am. Chem. Soc.* **2014**, 136, 1842–1855.

(75) Fukui, H.; Inoue, Y.; Yamada, T.; Ito, S.; Shigeta, Y.; Kishi, R.; Champagne, B.; Nakano, M. Enhancement of the Third-Order Nonlinear Optical Properties in Open-Shell Singlet Transition-Metal Dinuclear Systems: Effects of the Group, of the Period, and of the Charge of the Metal Atom. *J. Phys. Chem. A* **2012**, 116, 5501–5509.

(76) Yamada, T.; Inoue, Y.; Champagne, B.; Nakano, M. Theoretical Study on the Diradical Characters and Third-Order Nonlinear Optical Properties of Transition-Metal Heterodinuclear Systems. *Chem. Phys. Lett.* **2013**, 579, 73–77.

(77) Zhekova, H.; Seth, M.; Ziegler, T. Introduction of a New Theory for the Calculation of Magnetic Coupling Based on Spin–Flip Constricted Variational Density Functional Theory. Application to Trinuclear Copper Complexes which Model the Native Intermediate in Multicopper Oxidases. *J. Chem. Theory Comput.* **2011**, 7, 1858–1866.

(78) Rivero, P.; Moreira, I. de P. R.; Illas, F.; Scuseria, G. E. Reliability of Range Separated Hybrids Functionals in Describing Magnetic Coupling in Molecular Systems. *J. Chem. Phys.* **2008**, 129, 184110–184117.

(79) Reta Mañeru, D.; Pal, K. P.; Moreira, I. de P. R.; Datta, S. N.; Illas, F. The Triplet-Singlet Gap in the *m*-Xylylene Radical: A Not So Simple One. *J. Chem. Theory Comput.* **2014**, 10, 335–345.